

# Solid Texture Synthesis using Generative Adversarial Networks

Xin Zhao<sup>1</sup> Lin Wang<sup>1</sup> Jifeng Guo<sup>1</sup> Bo Yang<sup>1</sup> Junteng Zheng<sup>1</sup> Fanqi Li<sup>1</sup>

## Abstract

Solid texture synthesis, as an effective way to extend 2D texture to 3D solid texture, exhibits advantages in numerous application domains. However, existing methods generally suffer from synthesis distortion due to the underutilization of texture information. In this paper, we proposed a novel neural network-based approach for the solid texture synthesis based on generative adversarial networks, namely STS-GAN, in which the generator composed of multi-scale modules learns the internal distribution of 2D exemplar and further extends it to a 3D solid texture. In addition, the discriminator evaluates the similarity between 2D exemplar and slices, promoting the generator to synthesize realistic solid texture. Experiment results demonstrate that the proposed method can synthesize high-quality 3D solid texture with similar visual characteristics to the exemplar.

## 1. Introduction

Texture mapping, as a technique to enhance the visual effect of the object surface, is widely used in graphics applications (Haeberli & Segal, 1993; Earl et al., 2010). Currently, it usually requires a planar parameterization for mapping texture attributes to a 3D object. However, for complex textures, it is still a challenge to find a good planar parameterization (Kopf et al., 2007). The above is the domain of the surface texture. Contrasty, *solid texture* can describe textures directly from 3D space without planar parameterization. *Solid texture synthesis* attempts to learn a 3D solid texture generation process from a given 2D exemplar, and generates solid texture that has similar textural characteristics with the exemplar. It enables scientists to study 3D internal structures when only 2D examples are available (Turner & Kalidindi, 2016), and to aid medical assessment when imaging studies is expensive and may cause unreasonable high radiation for

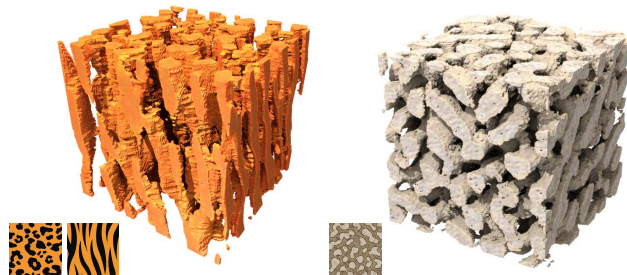


Figure 1. Exemplars of solid texture synthesized with STS-GAN. The left part illustrates the synthesized solid with anisotropic texture and the right is the isotropic case.

patient (Li et al., 2016).

As shown in Figure 1 which demonstrates the proposed method, the solid approach raises dimension for a 2D exemplar and projects its properties to a 3D object, not only the surface but also the whole volume. In terms of visual effects, a randomly taking slice from generated 3D solid texture shares similar or preferably same proprieties with the 2D exemplar.

The solid texture synthesis (Perlin, 1985; Peachey, 1985), starts with *procedural method* at an early age, requiring only a simple algorithm. Despite its advantages of efficiency and memory-saving, tuning parameters manually for a specific texture is burdensome. In addition, this type of model relies on human experiences, while humans only focus on prominent features in the texture, which may results in the lack of details and the failure of generating solid textures.

Compared with procedural method, the more recent *example-based models* (Heeger & Bergen, 1995; Jagnow et al., 2004; Kopf et al., 2007; Chen & Wang, 2010) are able to capture more details of texture and generate realistic solid texture. By matching strategies such as statistical information or similar neighborhoods, these methods produce solid textures approximating the texture characteristics of 2D exemplars in the orthogonal directions. However, these methods only take into account some manually extracted features, such as color and morphology, and do not take full advantage of the overall information of the texture, which

<sup>1</sup>Shandong Provincial Key Laboratory of Network Based Intelligent Computing, University of Jinan, Jinan 250022, China. Correspondence to: Lin Wang <wangplanet@gmail.com>, Bo Yang <yangbo@ujn.edu.cn>.

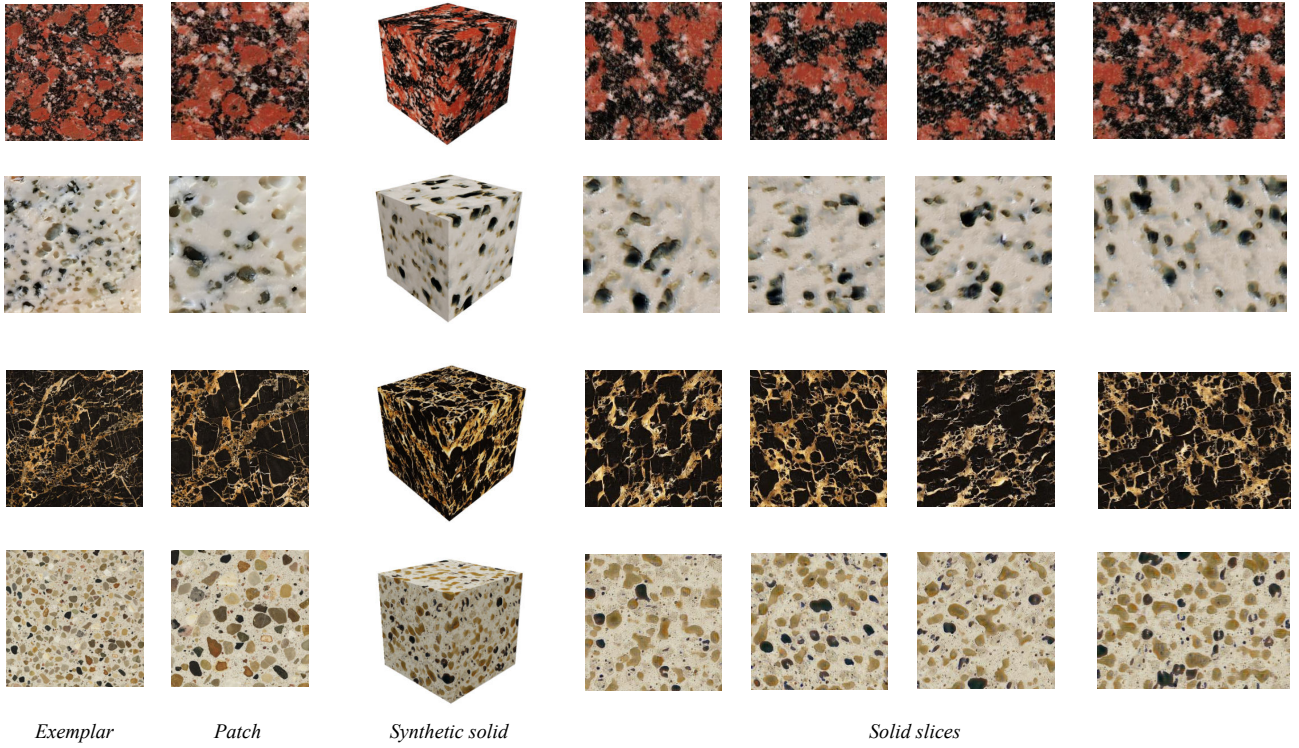


Figure 2. Solid texture synthesis based on isotropic exemplar. The first column illustrates isotropic exemplars with a resolution of  $512 \times 512$ . The second one is the randomly cropped patches ( $256 \times 256$ ) from the exemplar. The 3D solid texture ( $256^3$ ) generated by STS-GAN is shown in the third column. In addition, four slices of the generated solid across the three orthogonal directions and an oblique direction with a 45 angle are listed in the last part.

often results in distortion of the generated solid texture.

Taking advantage of the universal approximation ability, Gutierrez et al. (2018) introduced neural networks to synthesize solid texture, which can conceptualize many textures to synthesize objects with good visual results that are at least equivalent to the state-of-the-art approaches. Nevertheless, the feature extraction approaches can not be generalized to the universal set of textural distributions, which is still a hurdle at the front of current research.

*A question that arises here is: Can we design a model learning an arbitrary distribution of the 3D solid texture from a 2D exemplar?*

The Generative Adversarial Nets (GANs) (Goodfellow et al., 2014) have been proven to be able to capture arbitrary data distribution by adversarial learning and has received lots of successful stories in 2D texture synthesis (Bergmann et al., 2017; Shaham et al., 2019). In order to answer the aforementioned question, inspired by GANs, this study proposes a STS-GAN framework to synthesize 3D solid textures from 2D exemplars. In the framework, the generator learns the 2D textural distribution, and extends it to 3D objects. The

discriminator attempts to distinguish generated solid slices from the given exemplar. After the adversarial learning, the generative model is able to synthesize the 3D solids with similar textures corresponding to different exemplars.

This work makes the following major contributions.

- First time that the generative adversarial nets are introduced into solid texture synthesis.
- A multi-scale generative model is proposed to synthesize solid textural details at multi-scale levels.
- A discriminative model with pre-training module is adopted for accelerating convergence.

The rest of this paper presents the overview of the related work to solid texture synthesis in Section 2, describes our approach in detail in Section 3, and provides a demonstration of experimental results for various textures in Section 4.

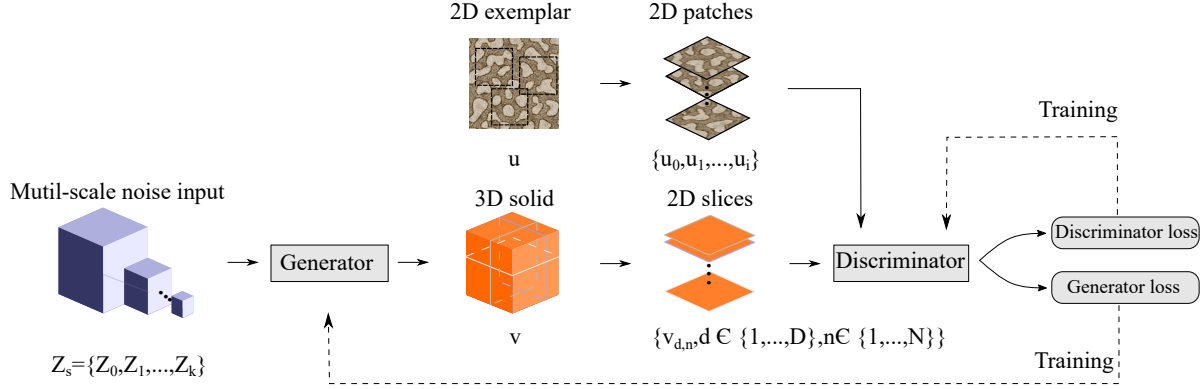


Figure 3. The whole framework for STS-GAN. Particularly, the generated solid texture  $v$  has a specified size  $(N \times N \times N)$ , where  $N$  can be set by the user. The 2D patches are randomly cropped from the 2D exemplar and the 2D slices are randomly selected from the synthesized 3D solid in multiple orthogonal directions  $D$ .

## 2. Related works

In computer graphics, texture is an important element to enrich the details of a 3D object surface. Catmull (1974) first introduced the concept of texture into computer graphics. He defined texture mapping as a method which applies texture attributes to a 3D object by using planar parameterization. Compared with solid texture synthesis, these methods only express the surface details of 3D objects which act like paintings and can not reconstruct the internal part. In addition, the texture mapping can not deal with the anisotropic textures which are widespread in reality.

Plenty of methods have been proposed to synthesize solid texture. Among them, procedural methods (Perlin, 1985; Peachey, 1985) were the earliest family with advantage of low computational cost. They synthesize textures by using a function of pixel coordinates and a set of manually tuning parameters. Perlin Noise (Perlin, 1985), perhaps the most widely used one, is a smooth gradient noise function which is used to create pseudo-random patterns by perturbing mathematical functions. The synthesized solid texture exhibits spatial consistency randomly. Nevertheless, finding a suitable set of parameters for a given image requires tedious trial-and-error. Furthermore, the existence of semantic gap prevents people from associating concepts, like marble or gravel, with accurate parameters.

Compared with procedural methods, example-based models are able to generate realistic solid texture because they could extract more details of textures from exemplars, instead of a accurate description. The pyramid histogram matching (Heeger & Bergen, 1995) method pioneered the work on solid texture synthesis from 2D exemplars. It matches the

texture appearance of a given digitized sample by the reproduces global statistics and further produces solid texture. Based on a spectral analysis of a 2D texture (digitized image) in various types, Ghazanfarpour and Dischler (1995) presented a solid texture generation method. Jagnow (2004) proposed a solid texture synthesis method based on stereoscopic techniques, which effectively preserves the structure of the texture. However, the color of the generated solids differs from the given exemplar due to segmentation.

Wei (2002) first applied a 2D neighborhood matching synthesis method to solid texture synthesis. Kopf et al. (2007) extended 2D texture optimization technique (Kwatra et al., 2005; Wexler et al., 2007) to synthesize 3D solid texture. In this method, the histogram matching forces the global statistics of the synthesized solid to match those of exemplars. Chen and Wang (2010) integrated position and index histogram matching into optimization framework with the k-coherence search, which effectively improve the quality of synthetic items. Although these methods can produce impressive results, they only take into account some statistics information, such as color and morphology, and do not take full advantage of the overall information of exemplars.

Gutierrez et al. (2018) introduced convolutional neural networks to synthesize solid texture, which can synthesize solid texture of arbitrary size that reconstruct the visual features of the exemplars along some directions. In their work, the image descriptor based on pre-training network can conceptualize various textures to synthesize solids with good visual results. However, this method can not be generalized to the universal set of textural distributions.



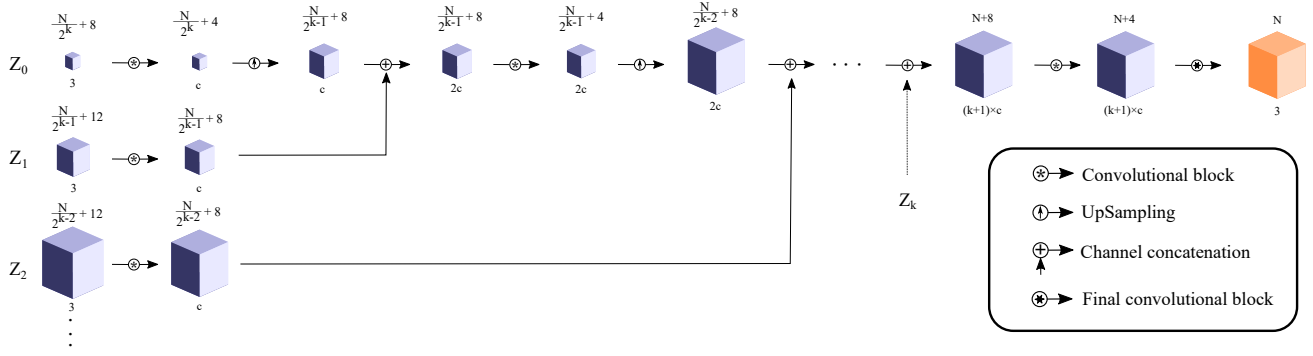


Figure 4. The structure of the solid texture generator. Especially, the upsampling in this model contains the nearest-neighbor interpolation and convolution.

### 3. STS-GAN

Generating solid texture from one single exemplar may have a shortage of information and further results in the failure of learning. Thus, inspired by (Bergmann et al., 2017), STS-GAN crops patches randomly from exemplars as real samples for the discriminator. Based on the assumption that if the 2D exemplar from a real 3D solid is similar to the slices from the synthesized 3D solid, then the synthesized 3D solid is equivalent to the real one, the orthogonal slices of the generated solid are fed into the discriminator as fake samples (Gutierrez et al., 2018) to correlate the 2D exemplar with the 3D solid texture. Importantly, this paper designs a multi-scale generator to synthesize solid textural details corresponding to different scales. Then all generated solids will be concatenated to the desired size.

As shown in Figure 3, the proposed STS-GAN consists of two parts: solid texture generator (STG) and slice texture discriminator (STD). Firstly, a group of multi-scale noise \$Z\_s\$ is fed into the solid texture generator which is responsible for reconstructing a 3D solid texture \$v\$. Then a set of slices \$v\_{d,n}\$ from the generated solid texture and a batch of image patches \$u\_i\$ from the 2D exemplar are distinguished by the slice texture discriminator. Specifically, the slices direction \$d\$ can be controlled which enables the generator to learn different textures in orthogonal directions. As a result, the model will have the ability to deal with anisotropic solid texture. During the adversarial learning, the STG devotes itself to generate 3D solid textures whose slices can confuse the STD, while the STD learns to discriminate slices from generated solid texture and the given exemplar as accurately as possible. After learning, the optimal generator is able to reconstruct realistic 3D solid texture.

#### 3.1. Solid Texture Generator

The generative model in STS-GAN adopts the idea of multi-scale. Notably, the generated multi-scale solids that do not

reach specified size, named temporary solids, are marked as \$TS\$.

As shown in Figure 4, the model contains \$K\$ (\$K = 1, 2, \dots, m\$) different scales. The multi-scale noises are first processed by a fixed convolutional block to form different lower scale temporary solids. In order to concatenate them together, lower scale needs to be expanded by upsampling. For example, after we get \$TS\_{\frac{N}{2^k}+8}\$ from \$Z\_0\$, we need to expand it to the size as same as the \$TS\_{\frac{N}{2^{k-1}}+12}\$ collected from \$Z\_1\$. Next, two temporary solids with same scale are concatenated in channels \$C\$. Finally, the fused temporary solid is processed by a final convolutional block to get a 3D solid with specified size (\$N \times N \times N\$). In the rest of this subsection, we will introduce those operations in detail.

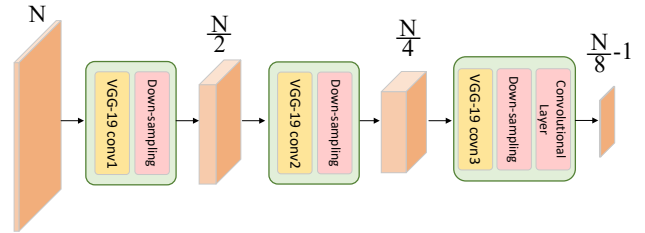


Figure 5. The structure for slice texture discriminator. Notably, the size of its input images \$N\$ is same as that of the 3D solid synthesised by the STG.

**Convolutional block** To refine texture in different scales, multi layers or kernels are designed in the convolutional blocks. In addition, the batch-normalization (BN) (Ioffe & Szegedy, 2015) and the leaky-relu are added to accelerate STG Training.

**Upsampling** Before concatenating solids with the same scale, the one with a lower scale must be extended to a large scale. Inspired by Augustus Odena et al. (2016), we adopt



Figure 6. The performance comparison of the model with Single scale and multi-scale.

the nearest-neighbor interpolation and convolution on image scaling. In interpolation, a 3D nearest neighbor is used, and the low scale solid will increase by 8 times.

**Final convolutional block** Lastly, the final convolutional block is introduced to map the temporary solid channels to the standard number, i.e., 3 channels.

### 3.2. Slice Texture Discriminator

Figure 5 details the slice texture discriminator. Inspired by (Bergmann et al., 2017), STD takes an image as input and gets a two-dimensional field as output. Each position of the two-dimensional field responds only to a local effective receptive field. The STD score is the mean of the two-dimensional field.

**Pre-training module** Since training a model from scratch by iterations takes a huge amount of time, a pre-training module is used in this paper to accelerate convergence. Previous studies have proven that using the VGG model (Simonyan & Zisserman, 2014) as a pre-training module achieves success in texture synthesis. Particularly, after trained with massive image data from ImageNet (Deng et al., 2009), VGG-19 possesses strong generalization capability. Therefore, this study adopts it as a pre-training module.

**Downsampling** Inspired by DCGAN (Radford et al., 2015), the STD use convolution with a stride size of 2 to replace the pooling layer, which allows it to extract features efficiently.

### 3.3. Adversarial Learning

In adversarial learning, the STG and STD trained alternately. The goal of STG is to generate realistic-looking texture that can not be discriminated as fake one by STD, while STD attempts to improve its discriminate ability to prevent

STG from reconstructing realistic texture. In this paper, the WGAN-GP (Gulrajani et al., 2017) loss is adopted because it can increase training stability.

When discriminator is optimized, the loss, computed by Eq.(1), is maximized.

$$\mathcal{L}_D = \mathbb{E}[D(v)] - \mathbb{E}[D(u)] + \lambda \mathbb{E}[(\|\nabla_r D(r)\|_2 - 1)^2] \quad (1)$$

where  $u$  is a randomly orthogonal 2D slice from the 3D solid produced by STG,  $v$  is a random patch from the exemplar, and  $r$  is a data point uniformly sampled along the straight line connecting  $v$  and  $u$ . After the STD possesses a good discriminate ability, the STG can be trained. Similarly, it is optimized by minimizing the generator loss function expressed by Eq.(2)

$$\mathcal{L}_G = \mathbb{E}[D(v)] \quad (2)$$



Figure 7. The performance of the STS-GAN for texture mapping on 3D mesh model. Source: The 3D mesh models come from Stanford 3D Scanning Repository.

## 4. Experiment

### 4.1. Settings

In this paper, the solid texture generator contains 3 different scales, i.e.,  $K = 3$ , while the multi-scales noise obey a

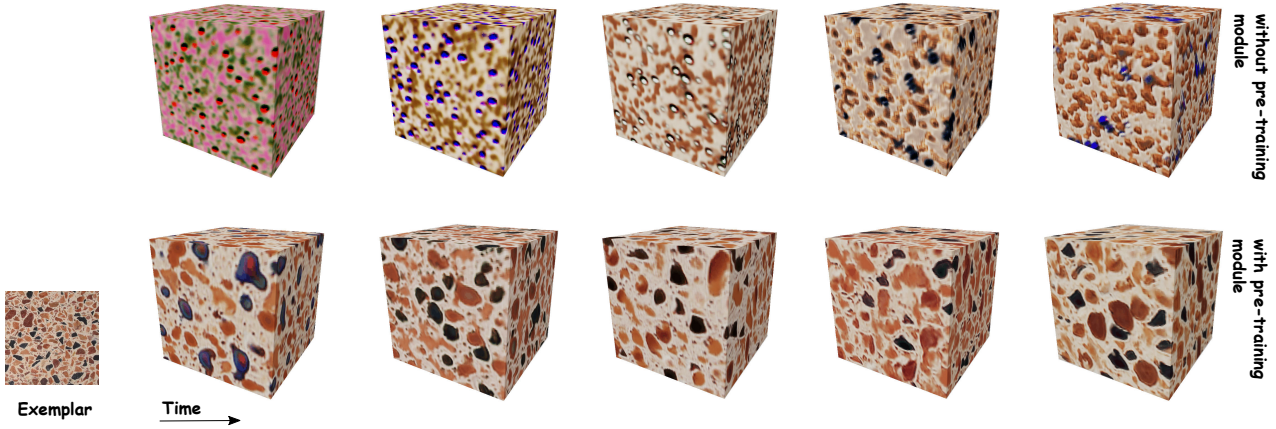


Figure 8. The performance comparison of the two models at different iterations, in which the STD with or without pre-training module.

normal distribution. The convolutional block consists of three 3D convolution layers, in which the size of the kernels is  $3 \times 3 \times 3$  for the first two layers and  $1 \times 1 \times 1$  for the last. The final convolutional block contains two convolutional layers with the kernel size of  $3 \times 3 \times 3$ . In the slice texture discriminator, the first three convolutional blocks of VGG-19 is used as pre-training modules and were fixed during the training process.

This framework is implemented by Pytorch. Training is performed with the Adam optimizer (Kingma & Ba, 2014), in which learning rate is 0.0005. In addition, this paper adopts a learning rate decay strategy that the learning rate is reduced to half of the original value each 8000 iterations. The batch size of the STG and STD are 1 and 32, respectively. All these parameters are tuned by trial and error. Based on the above settings, we need to spend about 20 hours to train a texture model (i.e., a patch with  $128 \times 128$  resolution) on one GPU Nvidia GeForce TITAN RTX.

#### 4.2. STG with Multi-scale

To demonstrate the advantage of using the multi-scale generator while learning textural distribution, STG with multi-scale noise is compared with one fed with single-scale noise. Both of them are used to generate 3D solid based on the same exemplar. Figure 6 illustrates the synthesized results using two models. Compared with the single-scale model, the multi-scale model can generate a higher quality solid texture with sufficient information. It learns the texture distribution of not only the whole properties but also the local details. Moreover, the 3D solid synthesized by the multi-scale model exhibits uniformity and consistency at different iterations, revealing its stability in learning textural distribution.

#### 4.3. STD with the Pre-training Model

In order to prove that using pre-training module is valid for improving the learning capability, models with and without pre-training module are tested using the same 2D exemplar. As shown in Figure 8, the 3D solid generated by the model with the pre-training module performs high consistency at each iteration, while the one without the pre-training module exhibits volatility to some extent. Particularly, the first solid generated by the latter is inconsistent with the 2D exemplar because its discriminator has a random parameter at first, which is not conducive to the generator’s learning. The results reveal that the STD with the pre-training module accelerating convergence and aids the STG to produce realistic solid texture.

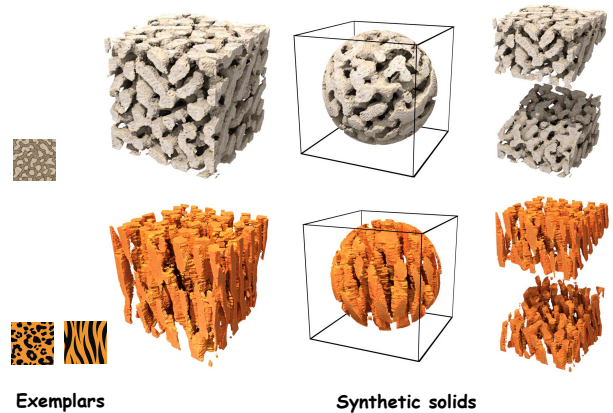


Figure 9. The interior texture in different views of the 3D solid synthesized by STS-GAN using the isotropic and anisotropic exemplar. Especially, to improve the display effect, this figure only shows the structure of one phase.



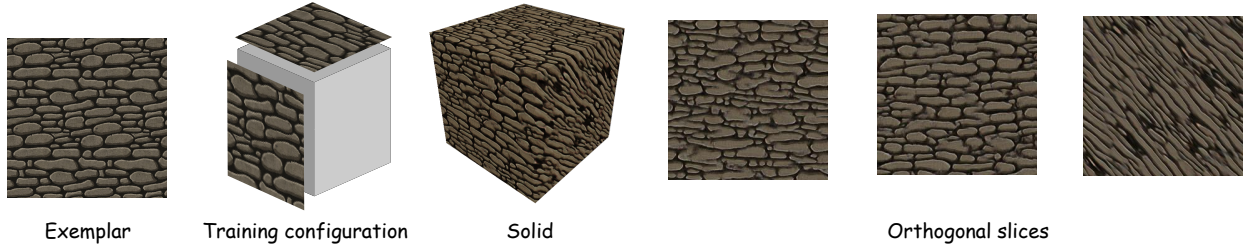


Figure 10. The synthetic effect of the STS-GAN with two constraint directions. The last part illustrates the synthetic solid slices in different orthogonal directions.

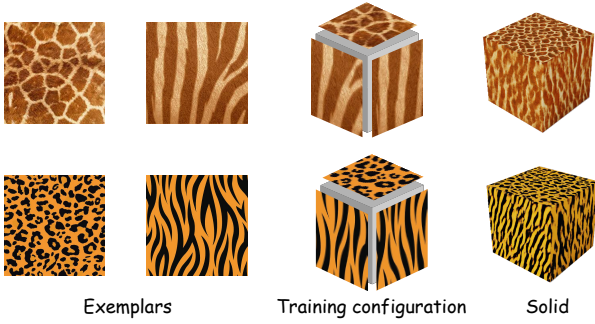


Figure 11. Result of the STS-GAN on the different anisotropic exemplars. In this model, two 2D images in different directions are required.

#### 4.4. STS-GAN for Texture Mapping

Compared with texture mapping, the solid texture synthesis also reconstructs texture for the entire volume. In this experiment, the STS-GAN is applied to texture mapping by using the synthesized solid. The pixels on the surface of the 3D mesh model are assigned by the synthesized solid based on the spatial coordinate information.

Figure 7 presents the results of STS-GAN on texture mapping. In terms of appearance, the texture on the 3D mesh model is in accordance with the 2D exemplar, which proves that the texture generated by STS-GAN presents regular texture even in irregular space. In addition, the generated solid texture can be repeatedly applied to different 3D mesh models.

#### 4.5. STS-GAN on the Isotropic exemplar

In this experiment, the proposed STS-GAN performs on different isotropic exemplars. As shown in Figure 2, the generated 3D solids are similar to the given 2D exemplars and patches. Besides, the slices from the 3D solid in different angles still keep the same textural characteristics as the exemplar. To further demonstrate the spatial consistency of

the generated solids, the interior texture in different views is also illustrated in Figure 9 (the top case). It can be found that the interior texture exhibits highly spatial consistency that there is no texture discontinuity for special views. This phenomenon reveals that STS-GAN has learned the accurate texture distribution, and effectively extended it to the 3D solids.

#### 4.6. STS-GAN on the Anisotropic exemplar

Since the STS-GAN learn the textural distribution from a 2D exemplar, it can generate 3D solid textures with anisotropic characteristics when the textures in different directions are given. In this experiment, based on the setting training configuration, which is shown in Figure 11, the STS-GAN are trained using two anisotropic exemplars in three different orthogonal directions.

As shown in Figure 11, despite subtle color diversion, the synthesized texture solids are highly consistent with two anisotropic exemplars. In addition, the interior texture in different views is also illustrated in Figure 9. It can be observed that the properties of anisotropic texture still exist and show continuity at different angles. These results indicate that STS-GAN enables learning anisotropic texture and extends it into a 3D solid.

#### 4.7. The Reasoning Ability of STS-GAN

Since the STS-GAN synthesizes the solid texture by learning the textural distribution from 2D exemplars, this experiment attempts to verify its reasoning ability on the direction with no constrain. As shown in Figure 10, the constrain acts in two directions. From the results, it can be found that the generated solid exhibits consistency in the constrained and unconstrained directions. Interestingly, there is no texture discontinuity between them. These results indicate that the proposed method does possess the reasoning ability on the unconstrained direction. It learns the distribution, not just the features, which could expand more reasonably and regularly.



Figure 12. The results comparison between the STS-GAN and the existing methods. The first line represents the simple texture and the last two lines are complex texture.

#### 4.8. Comparison with existing method

In this experiment, the STS-GAN is compared with the three existing methods, which seem to produce the best results: Kopf et al. (2007), Chen and Wang (2010) and Gutierrez et al. (2018).

Figure 12 illustrates some results obtained from another papers side by side with results using STS-GAN. For texture with single structure (in the first row), STS-GAN is able to capture more texture details, i.e., high frequency information, than that of Chen and Wang. For texture with complex structures (the second row), the proposed method, compared with the other three methods, shows great ability in preserving texture structure and richness. Nevertheless, for the last texture, solid texture generated by the STS-GAN contains some duplicate texture structure. This above phenomenon implies that the STS-GAN is difficult to learn complex textural information when the exemplar's size is small. The reason may due to the patches from the 2D exemplar only contains local information.

#### 5. Conclusion

In this paper, a novel approach STS-GAN is proposed to synthesize 3D solid texture from 2D exemplar. It is the first time that the generative adversarial nets are introduced into the field of solid texture synthesis. This method takes a multi-scale generative model to generate details at multi-scale levels. Moreover, the pre-training module is adopted in discriminator to accelerate convergence. Significantly, our method can reconstruct realistic solid textures from a given exemplar.

This work is the first attempt to open a brand new gate, associating solid texture synthesis with the powerful generative adversarial net. However, there is still room for improvement. A limitation is that the model is difficult to learn when the exemplar is small, because of the lack of information. The time consuming nature of neural networks also influences on real applications.

In future, in order to further improve discriminator, the multi-scale patch from exemplar and random angle slicing from synthesized textures are also required to augment data.



Furthermore, the generating process also needs to be accelerated to match real-time requirement in real applications.

## References

- Bergmann, U., Jetchev, N., and Vollgraf, R. Learning texture manifolds with the periodic spatial GAN. In Precup, D. and Teh, Y. W. (eds.), *Proceedings of the 34th International Conference on Machine Learning*, volume 70 of *Proceedings of Machine Learning Research*, pp. 469–477, International Convention Centre, Sydney, Australia, 06–11 Aug 2017. PMLR. URL <http://proceedings.mlr.press/v70/bergmann17a.html>.
- Catmull, E. A subdivision algorithm for computer display of curved surfaces. Technical report, UTAH UNIV SALT LAKE CITY SCHOOL OF COMPUTING, 1974.
- Chen, J. and Wang, B. High quality solid texture synthesis using position and index histogram matching. *The Visual Computer*, 26(4):253–262, 2010.
- Deng, J., Dong, W., Socher, R., Li, L.-J., Li, K., and Fei-Fei, L. Imagenet: A large-scale hierarchical image database. In *2009 IEEE conference on computer vision and pattern recognition*, pp. 248–255. Ieee, 2009.
- Earl, G., Martinez, K., and Malzbender, T. Archaeological applications of polynomial texture mapping: analysis, conservation and representation. *Journal of Archaeological Science*, 37(8):2040–2050, 2010.
- Ghazanfarpour, D. and Dischler, J.-M. Spectral analysis for automatic 3-d texture generation. *Computers & Graphics*, 19(3):413–422, 1995.
- Goodfellow, I., Pouget-Abadie, J., Mirza, M., Xu, B., Warde-Farley, D., Ozair, S., Courville, A., and Bengio, Y. Generative adversarial nets. In Ghahramani, Z., Welling, M., Cortes, C., Lawrence, N., and Weinberger, K. Q. (eds.), *Advances in Neural Information Processing Systems*, volume 27, pp. 2672–2680. Curran Associates, Inc., 2014. URL <https://proceedings.neurips.cc/paper/2014/file/5ca3e9b122f61f8f06494c97b1afccf3-Paper.pdf>.
- Gulrajani, I., Ahmed, F., Arjovsky, M., Dumoulin, V., and Courville, A. Improved training of wasserstein gans. *arXiv preprint arXiv:1704.00028*, 2017.
- Gutierrez, J., Rabin, J., Galerne, B., and Hurtut, T. On Demand Solid Texture Synthesis Using Deep 3D Networks. working paper or preprint, December 2018. URL <https://hal.archives-ouvertes.fr/hal-01678122>.
- Haeberli, P. and Segal, M. Texture mapping as a fundamental drawing primitive. In *Fourth Eurographics Workshop on Rendering*, volume 259, pp. 266. Citeseer, 1993.
- Heeger, D. J. and Bergen, J. R. Pyramid-based texture analysis/synthesis. In *Proceedings of the 22nd annual conference on Computer graphics and interactive techniques*, pp. 229–238, 1995.
- Ioffe, S. and Szegedy, C. Batch normalization: Accelerating deep network training by reducing internal covariate shift. In *International conference on machine learning*, pp. 448–456. PMLR, 2015.
- Jagnow, R., Dorsey, J., and Rushmeier, H. Stereological techniques for solid textures. *ACM Transactions on Graphics (TOG)*, 23(3):329–335, 2004.
- Kingma, D. P. and Ba, J. Adam: A method for stochastic optimization. *arXiv preprint arXiv:1412.6980*, 2014.
- Kopf, J., Fu, C.-W., Cohen-Or, D., Deussen, O., Lischinski, D., and Wong, T.-T. Solid texture synthesis from 2d exemplars. In *ACM SIGGRAPH 2007 papers*, pp. 2–es. 2007.
- Kwatra, V., Essa, I., Bobick, A., and Kwatra, N. Texture optimization for example-based synthesis. In *ACM SIGGRAPH 2005 Papers*, pp. 795–802. 2005.
- Li, Z., Desolneux, A., Muller, S., and Carton, A.-K. A novel 3d stochastic solid breast texture model for x-ray breast imaging. In *International Workshop on Breast Imaging*, pp. 660–667. Springer, 2016.
- Odena, A., Dumoulin, V., and Olah, C. Deconvolution and checkerboard artifacts. *Distill*, 1(10):e3, 2016.
- Peachey, D. R. Solid texturing of complex surfaces. In *Proceedings of the 12th annual conference on Computer graphics and interactive techniques*, pp. 279–286, 1985.
- Perlin, K. An image synthesizer. *ACM Siggraph Computer Graphics*, 19(3):287–296, 1985.
- Radford, A., Metz, L., and Chintala, S. Unsupervised representation learning with deep convolutional generative adversarial networks. *arXiv preprint arXiv:1511.06434*, 2015.
- Shaham, T. R., Dekel, T., and Michaeli, T. Singan: Learning a generative model from a single natural image. In *Proceedings of the IEEE/CVF International Conference on Computer Vision (ICCV)*, October 2019.
- Simonyan, K. and Zisserman, A. Very deep convolutional networks for large-scale image recognition. *arXiv preprint arXiv:1409.1556*, 2014.

- Turner, D. M. and Kalidindi, S. R. Statistical construction of 3-d microstructures from 2-d exemplars collected on oblique sections. *Acta Materialia*, 102:136–148, 2016. ISSN 1359-6454. doi: <https://doi.org/10.1016/j.actamat.2015.09.011>. URL <https://www.sciencedirect.com/science/article/pii/S1359645415006771>.
- Wei, L.-Y. *Texture Synthesis by Fixed Neighborhood Searching*. PhD thesis, Stanford, CA, USA, 2002. AAI3038169.
- Wexler, Y., Shechtman, E., and Irani, M. Space-time completion of video. *IEEE Transactions on pattern analysis and machine intelligence*, 29(3):463–476, 2007.